Density-correlation function for liquid helium near T_λ in the symmetric planar-spin model

P. C. Hohenberg
Bell Laboratories, Murray Hill, New Jersey 07974
and Physik Department, Technische Universität München, 8046 Garching, West Germany

E. D. Siggia*
Department of Physics, University of Pennsylvania, Philadelphia, Pennsylvania 19174

B. I. Halperin
Bell Laboratories, Murray Hill, New Jersey 07974
(Received 27 May 1976)

The density-correlation function $S(k,\omega)$ for liquid helium near T_λ is calculated in the symmetric planar-spin model in three dimensions, both above and below the transition. The approximation used is a self-consistent generalization of the lowest-order ϵ expansion, which resembles the mode-coupling expressions of Kawasaki and others. The spectrum is evaluated numerically for different values of $k\xi$, and predictions are made for the exponents and amplitudes of various singular dynamic quantities. The results are consistent with earlier ones based on an extrapolation of the second-order ϵ expansion. Comparison with experiment is possible without any adjustable parameters, and it is found that the results are consistent with existing measurements of the thermal conductivity, but inconsistent with the observed amplitude of second-sound damping. The results also disagree with light-scattering experiments at and below T_λ. These disagreements are at present unexplained.

I. INTRODUCTION

The critical dynamics of liquid helium near the superfluid transition may be investigated experimentally by macroscopic measurements of the thermal conductivity above T_λ,[1] and the damping of second sound below T_λ,[2] and by light-scattering experiments[3,4] at finite wave vector both above and below the transition. The phenomenological theory of dynamic scaling[5,6] has been quite successful in explaining the temperature dependence of the macroscopic quantities, but seems to disagree with the scattering experiments. Specifically, although the second-sound damping coefficient measured macroscopically increases as $T \to T_\lambda$ in accord with scaling predictions, no such variation was found in the light-scattering data.[3,4] An expected variation in the thermal-diffusion width above T_c is also absent from the light-scattering results.[4,7] The renormalization-group[8] approach to critical dynamics gives a microscopic justification for dynamic scaling, and in addition allows one to calculate, at least approximately, scaling functions and universal amplitude ratios[9] (Ref. 9, hereafter referred to as I). These determine the magnitude of the critically varying quantities and are clearly an important part of the comparison between experiment and theory. Estimates obtained in I from extrapolations of the ϵ expansion were in rough agreement with thermal-conductivity measurements above T_λ. A similar estimate[10] (Ref. 10, hereafter referred to as II) of the second-sound damping in the hydrodynamic region below T_λ, given in II, was found to be smaller than the experimental values by a factor[11] ≈ 5.

The present paper applies the renormalization-group method in three dimensions to an approximate calculation of the density-correlation function $S(k, \omega)$ near the transition, based on the symmetric planar model (E) introduced in I. Calculations are performed both above and below T_λ, for various values of $k\xi$, in order to permit comparison with the light-scattering measurements. The approximation used is a self-consistent generalization to three dimensions of the first-order ϵ expansion valid near four dimensions.[9,10] The resulting expressions are analogous to those of the mode-coupling theory,[12-14] which had been solved earlier at T_c by Wegner[15] and Joukoff,[16] for the case of an isotropic antiferromagnet. Below T_c we have included *dissipative* coupling[9] between modes, in addition to the nondissipative mode-coupling terms usually considered.[12-16] In principle, such dissipative terms appear also at and above T_c, but not in first order, so that our approximation corresponds precisely to the mode-coupling equations in that case. The generalization to temperatures below T_c involves considerably more complicated expressions than at and above T_c, and we have made further simplifications in obtaining numerical solutions. We estimate the final accuracy of our model calculations to be of the order of a factor of 2 or better in the dimensionless ratios and scaling functions.

The results are consistent with those obtained earlier[9,10] on the basis of the ϵ expansion, and

therefore only agree with experiment above T_c and at long wavelengths. In the hydrodynamic region below T_c we again underestimate the damping of second sound by a factor of 5.[11] In the light-scattering regime, our theory would predict measureable temperature dependence in the width of the second-sound and thermal-diffusion peaks, and no such variation has been observed. Although a detailed comparison between experiment and theory remains to be carried out, it seems unlikely to us that the symmetric planar-spin model will explain the light-scattering data, even qualitatively. A possible explanation of the discrepancy below T_λ is the existence of slow relaxation processes associated with the temperature dependence of the specific heat. Although these terms are absent in the symmetric model, they appear as slow "transients" in the more realistic asymmetric planar-spin system (model F of I), and may well have to be considered. It is unlikely, however, that these terms could explain the apparent discrepancy at and above T_λ.

Section II contains a description of the self-consistent equations and the resulting frequency spectrum for arbitrary values of k and ξ. The full correlation function is calculated in the symmetric planar-spin model, with no adjustable parameters. In Sec. III the results are applied to superfluid helium. The nonuniversal frequency scale is determined at each pressure by fitting to the measured second-sound velocity below T_λ, and the scale of lengths is obtained from other measurements, as discussed previously.[17] The effects of departures from the symmetric model are discussed briefly, but no calculations are carried out in the asymmetric model.

II. DERIVATION OF THE SELF-CONSISTENT EQUATIONS

We start from the equations of motion for the symmetric model (E) of I, for $T \leq T_c$

$$\frac{\partial m}{\partial t} = \lambda_0 \nabla^2 \frac{\delta F_0}{\delta m} - g_0 \psi_0 \frac{\delta F_0}{\delta \psi_T} + g_0 \left(\psi_T \frac{\delta F_0}{\delta \psi_L} - \psi_L \frac{\delta F_0}{\delta \psi_T} \right) + \zeta , \tag{2.1}$$

$$\frac{\delta \psi_L}{\delta t} = -\Gamma_0 \frac{\delta F_0}{\delta \psi_L} - g_0 \psi_T \frac{\delta F_0}{\delta m} + \theta_L , \tag{2.2}$$

$$\frac{\delta \psi_T}{\delta t} = -\Gamma_0 \frac{\delta F_0}{\delta \psi_T} + g_0 \psi_0 \frac{\delta F_0}{\delta m} + g_0 \psi_L \frac{\delta F_0}{\delta m} + \theta_T . \tag{2.3}$$

We have rewritten the complex field ψ of I in terms of the average order parameter

$$\psi_0 \equiv \langle \psi \rangle , \tag{2.4}$$

and the real fields ψ_L and ψ_T as

$$\psi = \psi_0 + \psi_L - i\psi_T . \tag{2.5}$$

The free energy F_0 is

$$F_0 = \int d^d x \{ (r_0 + 4u_0\psi_0^2)\psi_0\psi_L + \tfrac{1}{2}[(r_0 + 12u_0\psi_0^2)\psi_L^2 + (\nabla\psi_L)^2] + \tfrac{1}{2}[(r_0 + 4u_0\psi_0^2)\psi_T^2 + (\nabla\psi_T)^2] + \psi_L(\psi_L^2 + \psi_T^2)4u_0\psi_0 + (\psi_L^2 + \psi_T^2)^2 u_0 + \tfrac{1}{2}\chi_0^{-1} m^2 \} , \tag{2.6}$$

and the noise sources obey the equations

$$\langle \theta_L(x,t)\theta_L(x',t') \rangle = 2\Gamma_0 \delta(x-x')\delta(t-t') , \tag{2.7}$$

$$\langle \theta_T(x,t)\theta_T(x',t') \rangle = 2\Gamma_0 \delta(x-x')\delta(t-t') , \tag{2.8}$$

$$\langle \zeta(x,t)\zeta(x',t') \rangle = -2\lambda_0 \nabla^2 \delta(x-x')\delta(t-t') , \tag{2.9}$$

$$\langle \theta_L \theta_T \rangle = \langle \theta_L \zeta \rangle = \langle \theta_T \zeta \rangle = 0 . \tag{2.10}$$

We wish to calculate the dynamic correlation functions for the fields m, ψ_L and ψ_T self-consistently to the lowest nontrivial order in the vertices g_0, u_0, and $u_0\psi_0$. This means that we expand the equations of motion up to order g_0^2, u_0, $(u_0\psi_0)^2$, and $(g_0 u_0 \psi_0)$. Invoking (2.4), we write the free energy to the necessary order as

$$F_0 = \int d^d x \{ \tfrac{1}{2}[\bar{\kappa}_0^2 \psi_L^2 + (\nabla\psi_L)^2] + \tfrac{1}{2}(\nabla\psi_T)^2 + \tfrac{1}{2}\chi_0^{-1} m^2 + 4u_0\psi_0\psi_L(\psi_L^2 + \psi_T^2) \} , \tag{2.11}$$

where

$$\bar{\kappa}_0^2 = r_0 + 12u_0\psi_0^2 = 8u_0\psi_0^2 . \tag{2.12a}$$

We shall eventually replace $\bar{\kappa}_0$ and u_0 by renormalized quantities $\bar{\kappa} \propto (T_c - T)^\nu$ and $u \propto \bar{\kappa}^{4-d}$, such that

$$\bar{\kappa}^2 = 8u\psi_0^2 , \tag{2.12b}$$

and $\psi_0^2 \propto \bar{\kappa}^{d-2}$. The dynamic correlation functions may now be obtained by a perturbation expansion of the equations of motion. We have used the formalism described in I, which necessitates the introduction of auxiliary fields $\hat{\psi}_L$, $\hat{\psi}_T$, and $\hat{m}$, and a large number of self-energies, coupled together by matrix equations. The general structure of the self-energy diagrams is as shown in Fig. 1, where the vertices are g_0 or $u_0\psi_0$, and the propagators involve the coupled fields ψ_T and m, and their adjoints, or ψ_L and its adjoint.[9] The fully self-consistent equations are therefore coupled nonlinear integral equations involving a large number of such correlation and response functions. In order to obtain a manageable theory we have made a number of approximations to these integral equations by choosing simple forms with free parameters for the intermediate propagators. The pa-

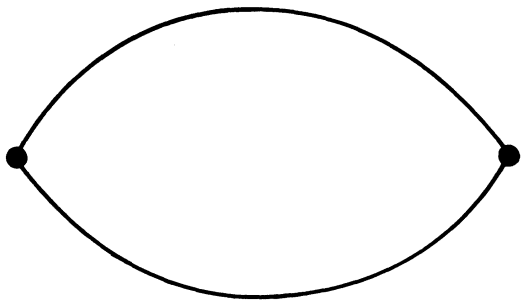

FIG. 1. Self-energy diagram contributing to the lowest-order self-consistent approximation. At and above T_c the vertex is g_0, and the solid lines represent matrix propagators involving the fields ψ and m and their "adjoints" $\hat{\psi}$, $\hat{m}$. Below T_c there is an additional vertex $u_0\psi_0$, and the propagators involve the fields ψ_L, ψ_T, $\hat{\psi}_L$, and $\hat{\psi}_T$, as well as m and $\hat{m}$.

rameters were then fixed by various self-consistency conditions.

A. Case $T = T_c$

Let us illustrate our general procedure by specializing to the case $T = T_c$, $(\bar{\kappa} = 0)$, where the equations simplify considerably. We begin by considering the more general case $T \geq T_c$, where we need only retain the vertex g_0, since $\psi_0 = 0$, and u_0 does not enter the dynamics in linear order. The self-consistent equations for the correlation functions for $T \geq T_c$ are [see Eqs. (B4), (B7), and (B15) of I]

$$C_m(k,\omega) = C_{mm} = D_{11} = 2\chi_m \,\mathrm{Re} D_{12}(k,\omega)\,, \tag{2.13a}$$

$$\tfrac{1}{2}C_{\psi\psi^*}(k,\omega) = \tfrac{1}{2}G_{11} = 2\chi_\psi(k)\,\mathrm{Re}G_{12}(k,\omega)\,, \tag{2.13b}$$

$$D_{12}(k,\omega) = [-i\omega + \lambda_0 k^2 \chi_m^{-1} - \Pi_{21}(k,\omega)]^{-1}\,, \tag{2.14a}$$

$$G_{12}(k,\omega) = [-i\omega + \Gamma_0 \chi_\psi^{-1}(k) - \Sigma_{21}(k,\omega)]^{-1}\,, \tag{2.14b}$$

$$\Pi_{21}(k,\omega) = -\chi_m^{-1} g_0^2 \int \frac{d^d p}{(2\pi)^d}\frac{d\omega'}{2\pi}\,[\chi_\psi^{-1}(p) - \chi_\psi^{-1}(p+k)]^2 \times \chi_\psi(p+k)\chi_\psi(p) \times [G_{12}(p+k,\omega-\omega')G_{12}(p,\omega')]\,, \tag{2.15a}$$

$$\Sigma_{21}(k,\omega) = -\chi_\psi^{-1}(k)\chi_m^{-1} g_0^2 \int \frac{d^d p}{(2\pi)^d}\frac{d\omega'}{2\pi}\chi_\psi(p) \times D_{12}(k+p,\omega-\omega')G_{12}(p,\omega')\,. \tag{2.15b}$$

We now make the Ornstein-Zernike approximation

$$\chi_\psi(k) = (\kappa_+^2 + k^2)^{-1}\,, \tag{2.16a}$$

$$\chi_m(k) = \chi_0\,, \tag{2.16b}$$

where $\kappa_+ = \xi_+^{-1}$ is the inverse correlation length above T_c. The above equations correspond precisely to the ones written down by Kawasaki[13] for the case of model G (the isotropic antiferromagnet), and they have been solved numerically in that case by Wegner[15] and Joukoff[16] as function of κ and ω, for $T = T_c$. [For the antiferromagnet the right-hand side of (2.15b) is multiplied by 2.]

Instead of repeating this calculation we have made approximations to the functions appearing in the integrals (2.15), since similar approximations are necessary below T_c. Let us note that for $T = T_c(\kappa_+ = 0)$, Eqs. (2.14)–(2.15) possess a self-consistent solution with the scaling form

$$\Pi_{21}(k,\omega) = A_\infty k^{3/2}\sigma_m(\omega/A_\infty q^{3/2})\,, \tag{2.17a}$$

$$\Sigma_{21}(k,\omega) = B_\infty k^{3/2}\sigma_\psi(\omega/B_\infty q^{3/2})\,, \tag{2.17b}$$

if we neglect the terms in λ_0 and Γ_0 in Eqs. (2.14) [these terms are small (of order k^2) compared to the terms in Σ and Π, which are of order $k^{3/2}$]. The approximation we shall make for the intermediate propagators is to neglect the frequency dependence in (2.17), i.e., we assume a Lorentzian spectrum with

$$\Pi_{21}(k,\omega) = A_\infty k^{3/2}\,, \tag{2.18a}$$

$$\Sigma_{21}(k,\omega) = B_\infty k^{3/2}\,, \tag{2.18b}$$

and determine the parameters A_∞ and B_∞ by a self-consistency requirement. Specifically, we calculate the "median frequencies"[18] of C_{mm} and $C_{\psi\psi^*}$ using (2.18) in (2.14) and (2.15), for given values of A_∞ and B_∞, and require that these medians be equal to (2.18a) and (2.18b), respectively. The ensuing values of A_∞ and B_∞ are expressible in terms of the dimensionless ratios

$$R_\lambda^\infty \equiv \chi_0^{1/2} A_\infty / g_0\,, \tag{2.19}$$

$$R_\Gamma^\infty \equiv \chi_0^{1/2} B_\infty / g_0\,, \tag{2.20}$$

which take on the self-consistent values

$$R_\lambda^\infty = 0.34\,, \quad R_\Gamma^\infty = 0.25\,. \tag{2.21}$$

In order to obtain manageable equations in the calculation below T_c, it was necessary to make the additional approximation

$$A_\infty = B_\infty\,, \tag{2.22}$$

so we have also solved (2.13)–(2.18) with this restriction, by requiring that the geometric mean of the median frequencies of C_{mm} and $C_{\psi\psi^*}$ be given self-consistently. The value obtained is

$$R_\lambda^\infty = R_\Gamma^\infty = 0.28\,, \tag{2.23}$$

which is rather close to the geometric mean of the numbers in (2.21).

B. Case $T < T_c$

As explained above, in the ordered phase there are two additional vertices, $u_0\psi_0$ and u_0, and many additional correlation and response functions. We have made the Lorentzian approximation in the intermediate propagators by choosing the correlation functions of the form

$$C_L(q,\omega) = \langle \psi_L \psi_L \rangle(q,\omega) = \frac{2\bar{\Gamma}}{\omega^2 + \bar{\Gamma}^2(\bar{\kappa}^2 + q^2)^2}\,, \tag{2.24}$$

$$C_m(q,\omega) = \langle mm \rangle(q,\omega) = \frac{2\bar{\lambda}q^2\,|-i\omega + \bar{\Gamma}q^2|^2 + 2\bar{\Gamma}q^2\chi_0 u_2^2 q^2}{\Delta}\,, \tag{2.25}$$

$$C_T(q,\omega) = \langle \psi_T \psi_T \rangle(q,\omega) = \frac{2\bar{\Gamma}\,|-i\omega + \bar{\Gamma}q^2|^2 + 2\bar{\Gamma}u_2^2 q^2}{\Delta}\,, \tag{2.26}$$

$$\langle \psi_T m \rangle(q,\omega) = \frac{4i\omega\bar{\Gamma}g_0\psi_0 q^2}{\Delta}\,, \tag{2.27}$$

$$\Delta = |(-i\omega + \chi_0^{-1}\bar{\lambda}q^2)(-i\omega + \bar{\Gamma}q^2) + u_2^2 q^2|^2\,, \tag{2.28}$$

with corresponding formulas for the other response functions which arise in our formalism. The quantities $\bar{\Gamma}$ and $\bar{\lambda}$ are for the moment arbitrary functions of k and $\bar{\kappa}$, but are independent of ω. We shall, however, impose the additional approximation

$$\chi_0^{-1}\bar{\lambda} = \bar{\Gamma}\,. \tag{2.29}$$

Similarly, in Eqs. (2.24)–(2.25), the approximation was made that the same $\bar{\Gamma}$ occurs in the longitudinal and transverse functions.

With the above ansatz for the intermediate propagators, a long but straightforward expansion of the equations of motion up to order g_0^2, $u\psi_0 g_0$ and u yields the expressions

$$\chi_0^{-1}C_m(k,\omega) = \frac{(2\lambda_0 k^2 + 2\chi_0\,\mathrm{Re}\,\Sigma_1)\,|-i\omega + \Gamma_0\chi_T^{-1} + \Sigma_2|^2 + (2\Gamma_0\chi_T^{-1} + 2\,\mathrm{Re}\,\Sigma_2)g_0^2\psi_0^2\chi_T^{-1}}{|(-i\omega + \lambda_0\chi_0^{-1}k^2 + \Sigma_1)(-i\omega + \Gamma_0\chi_T^{-1} + \Sigma_2) + g_0^2\chi_0^{-1}\psi_0^2\chi_T^{-1}|^2}\,, \tag{2.30}$$

$$\Sigma_1(k,\omega) = g_0^2\chi_0^{-1}\int \frac{d^dq}{(2\pi)^d}\,\frac{(q_+^2 - q_-^2)^2}{q_-^2(\bar{\kappa}^2 + q_+^2)}\left(\frac{-i\omega + L}{D}\right)\,, \tag{2.31}$$

$$\Sigma_2(k,\omega) = g_0^2\chi_0^{-1}\int \frac{d^dq}{(2\pi)^d}\left(\frac{-i\omega + L}{D(\bar{\kappa}^2 + q_+^2)}\right) - 8u\bar{\Gamma}(k)k^2\int \frac{d^dq}{(2\pi)^d}\left(\frac{2u_2^2q_-^2 + \bar{\Gamma}(q_-)\bar{\kappa}^2(-i\omega + L)}{q_-^2(\bar{\kappa}^2 + q_+^2)D}\right)$$
$$- 16u[-i\omega + \bar{\Gamma}(k)k^2]\int \frac{d^dq}{(2\pi)^d}\left(\frac{(q_+^2 - q_-^2)[u_2^2q_-^2 + \bar{\Gamma}(q_-)\bar{\kappa}^2(-i\omega + L)]}{\bar{\kappa}^2q_-^2(\bar{\kappa}^2 + q_+^2)D}\right)\,, \tag{2.32}$$

$$\chi_T^{-1} = k^2 + 8u\bar{\kappa}^2\int \frac{d^dq}{(2\pi)^d}\left(\frac{1}{q_-^2(\bar{\kappa}^2 + q_+^2)} - \frac{1}{q^2(\bar{\kappa}^2 + q^2)}\right)\,, \tag{2.33}$$

$$\vec{q}_\pm = \vec{q} \pm \tfrac{1}{2}\vec{k}\,, \tag{2.34}$$

$$L = \bar{\Gamma}(q_-)q_-^2 + \bar{\Gamma}(q_+)(\bar{\kappa}^2 + q_+^2)\,, \tag{2.35}$$

$$D = (-i\omega + L)^2 + u_2^2q_-^2\,, \tag{2.36}$$

with

$$u_2^2 = g_0^2\chi_0^{-1}\kappa_T^{d-2} = g_0^2\chi_0^{-1}\xi_T^{2-d} \approx g_0^2\chi_0^{-1}\psi_0^2\,. \tag{2.37}$$

(Note that $\kappa_T \equiv \xi_T^{-1}$ was denoted κ_- in I.) In obtaining Eqs. (2.30)–(2.37) we have freely used Eqs. (2.12b) and (2.29). Near four dimensions Eq. (2.30) reduces to Eq. (1) of II, with $\bar{\Gamma}$ independent of k and $\bar{\kappa}$. In three dimensions we shall make the scaling ansatz

$$\chi_0^{-1}\bar{\lambda} = \bar{\Gamma}(q,\bar{\kappa}) = A_-(\bar{\kappa}^2 + a_-^2q^2)^{-1/4}\,, \tag{2.38}$$

which involves one additional parameter, since a_- and A_- are related to the T_c value A_∞ of (2.18a) by

$$A_\infty = A_-a_-^{-1/2}\,. \tag{2.39}$$

When Eq. (2.38) is used for $\bar{\Gamma}$, it may be verified once again that the self-energies Σ_1 and Σ_2 scale as $k^{3/2}$, so for small k or $\bar{\kappa}$ we may neglect the terms in Γ_0 and λ_0 in Eq. (2.30) for $C_m(k,\omega)$. We shall therefore set

$$\Gamma_0 = \lambda_0 = 0\,, \tag{2.40}$$

in calculating the asymptotic expression for the correlation function. Let us set the frequency scale in (2.30) by

$$\Omega_\infty = A_\infty k^{3/2}\,, \tag{2.41}$$

and the length scale by ξ_T. Then it may be seen that $C_m(k,\omega)$ is entirely determined as a function of the reduced variables ω/Ω_∞ and $k\xi_T$ by the parameters $\bar{\kappa}\xi_T, a_-$ [Eq. (2.38)], and the dimensionless vertex

$$\bar{g}^2 = g_0^2/2\pi^2\chi_0A_-^2 = g_0^2/2\pi^2\chi_0A_\infty^2a_-$$
$$= 1/2\pi^2(R_\Gamma^\infty)^2a_- = u_2^2\xi_T/2\pi^2A_-^2\,. \tag{2.42}$$

The parameter R_Γ^∞ was already determined at T_c [Eq. (2.21)], so there are only two further parmeters. The first of these, $\bar{\kappa}\xi_T$, is a purely static

parameter, since from Eq. (2.24) we see that in the present approximation the static longitudinal correlation function is given by

$$C_L(q) = (q^2 + \bar{\kappa}^2)^{-1} . \tag{2.43}$$

It is known[19] that this approximation is not accurate as $q \to 0$, but we are interested in $C_L(q)$ for finite q, of order ξ_T^{-1}, and Eq. (2.43) is to be considered a simple parametrization of this function. Given an expression for $C_L(q)$ we could fit it to (2.43) and thus determine $\bar{\kappa}$. In the limit $d \to 4$ Eq. (2.43) becomes correct and we find

$$(\bar{\kappa}\xi_T)_{d\to 4} = (5K_4/\epsilon)^{1/(\epsilon-2)} . \tag{2.44}$$

Since we do not at present have a reliable expression for $C_L(q)$ in three dimensions, we shall extract $\bar{\kappa}$ from experiments. Specifically, we shall assume that $\bar{\kappa}^{-1}$ is the healing length ξ_H, which determines the depression of T_c in finite geometries.[20] This length has been measured in helium, and is equal to[20]

$$\xi_H = 1.2\{[T_\lambda(P) - T]/T_\lambda(P)\}^{-0.67} \text{ Å} \tag{2.45a}$$

at all pressures. The transverse correlation length ξ_T has also been measured,[17]

$$\xi_T = 3.57\{[T_\lambda(P) - T]/T_\lambda(P)\}^{-0.67} \text{ Å} , \tag{2.45b}$$

so the ratio is

$$\bar{\kappa}\xi_T = \xi_T/\xi_H = 3.0 . \tag{2.46}$$

The only remaining parameter is a_-, which we determine by requiring approximate self-consistency of $C_m(k, \omega)$ below T_c. We have evaluated Eq. (2.30) numerically for $k\xi_T = 1.5$ as a function of ω/Ω_∞, for different values of a_- in Eq. (2.38), with the other parameters fixed by Eqs. (2.23), (2.46), and (2.42). The resultant value of $\bar{\Gamma}$ was found by setting the full-width at half-maximum of the second-sound peak equal to $2\bar{\Gamma}k^2$ [see (2.24) and (2.29)]. For self-consistency this value of $\bar{\Gamma}$ was required to agree with Eq. (2.38), with the same value of a_-. The result is

$$a_- = 0.32 . \tag{2.47}$$

In this way the correlation function $\chi_0^{-1}C_m(k, \omega)$ is completely determined as a function of $k\xi_T$ and ω/Ω_∞. The correlation length ξ_T is known from measurements of ρ_s,[17] and the nonuniversal frequency scale Ω_∞ is fixed by fitting to the measured second-sound velocity for $k\xi_T \to 0$ [cf. Eq. (2.42)],

$$A_\infty = R_\Gamma^\infty u_2 \xi_T^{1/2} . \tag{2.48}$$

C. Case $T > T_c$

For $T > T_c$ the starting equations are (2.13)–(2.16), and the approximate Π_{21} is given by

$$\Pi_{21}(k, \omega) = g_0^2\chi_0^{-1}\int \frac{d^dq}{(2\pi)^d}\frac{q_+^2 - q_-^2}{(q_-^2 + \kappa_+^2)(q_+^2 + \kappa_+^2)} \times [-i\omega + \bar{\Gamma}(q_+)(\kappa_+^2 + q_+^2) + \bar{\Gamma}(q_-)(\kappa_+^2 + q_+^2)]^{-1} , \tag{2.49}$$

with $\vec{q}_\pm = \vec{q} \pm \vec{k}/2$. We now make the ansatz

$$\bar{\Gamma}(q) = A_+(\kappa_+^2 + a_+^2q^2)^{-1/4} , \tag{2.50}$$

with

$$A_\infty = A_+a_+^{-1/2} . \tag{2.51}$$

The new parameters are thus ξ_+ and a_+. The former was discussed in Ref. 17 where it was determined, from specific-heat measurements in helium and series expansions, to be equal to

$$\xi_+ = \kappa_+^{-1} = 1.41\{[T - T_\lambda(P)]/T_\lambda(P)\}^{-0.67} \text{ Å} . \tag{2.52}$$

The parameter a_+ is determined by self-consistency on the half-width at half-maximum of (2.14b), and the value obtained is

$$a_+ = 0.47 , \tag{2.53}$$

when A_∞ is given by (2.19) and (2.23).

III. RESULTS AND DISCUSSION

A. Results for the symmetric model

Numerical results for $\chi_0^{-1}C_m(k, \omega)$ as a function of ω/Ω_∞ are shown in Fig. 2, for representative values of $k\xi_T$ ($T < T_c$) and $k\xi_+$ ($T > T_c$). The qualitative behavior is as expected from dynamic scaling,[5,6] with second sound gradually broadening and merging into a single peak at and above T_c. The most interesting quantitative features are that second sound retains its "propagating" character up to $k\xi_T \approx 10$, and that the spectrum at T_c has significant departures from a Lorentzian shape. The fact that the latter spectrum has its maximum at $\omega \neq 0$ may be an artifact of our approximation, however. Similar features were found in earlier studies of the antiferromagnet at T_c.[15,16,21] The results may be summarized by evaluating a number of the dimensionless ratios defined in I and II. The parameter R_λ of I is equal to

$$R_\lambda \equiv \lim_{T\to T_c^+}(\bar{\lambda}\xi_+^{-1/2}/g_0\chi_0^{1/2}) = R_\lambda^\infty a_+^{1/2} = 0.19 , \tag{3.1}$$

whereas the corresponding values at T_c are given by

$$R_\lambda^\infty = 0.28 , \tag{3.2}$$

$$R_\Gamma^\infty = 0.28 , \tag{3.3}$$

with the constraint (2.22), and

$$R_\lambda^\infty = 0.34 , \tag{3.2a}$$

$$R_\Gamma^\infty = 0.25 , \tag{3.3a}$$

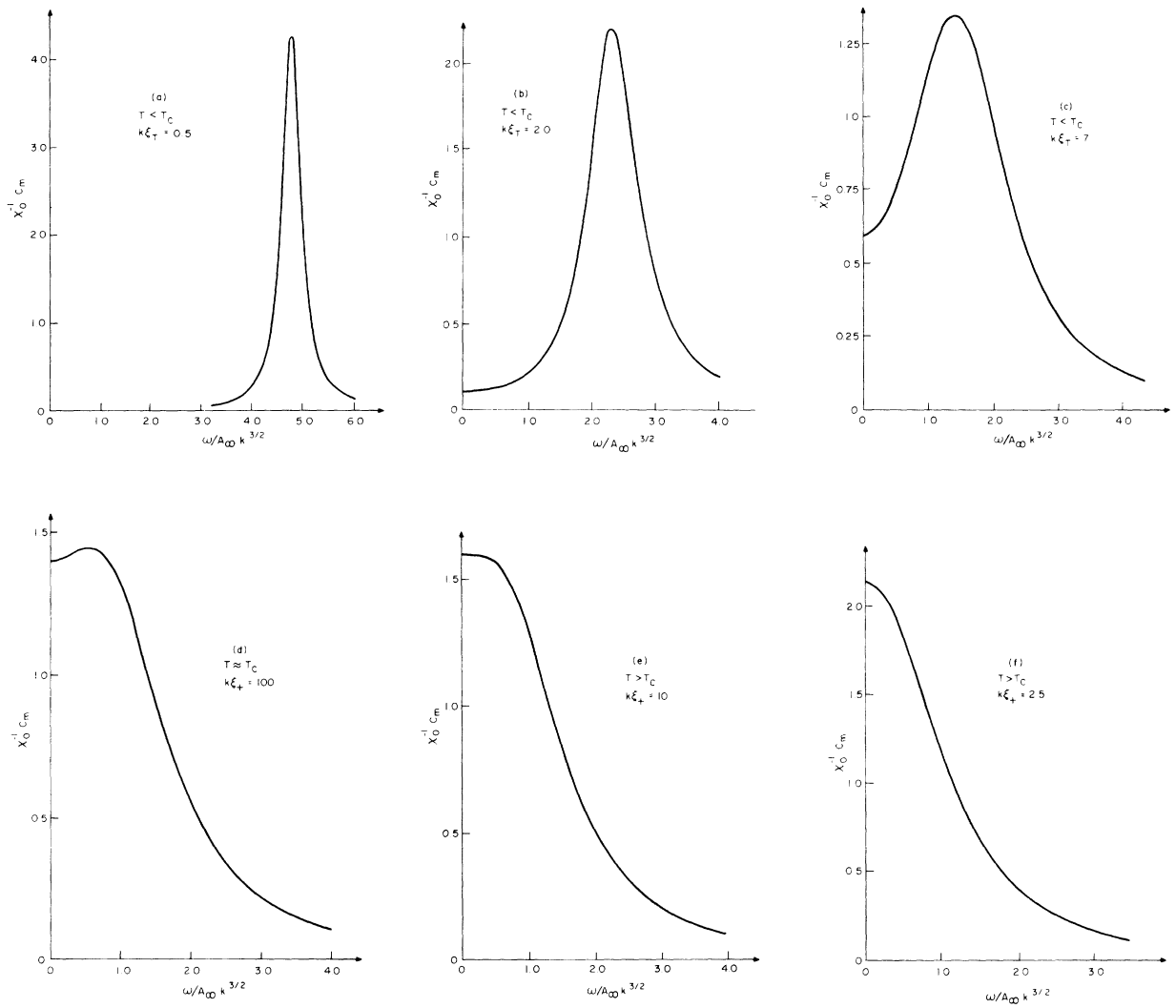

FIG. 2. The correlation function $\chi_0^{-1}C_m(k,\omega)$ which is proportional to $S(k,\omega)$, plotted as a function of the reduced frequency $\omega/A_\infty k^{3/2}$, for fixed values of $k\xi$. The function is only shown for positive ω, and it has been normalized so that its integral from 0 to ∞ is π. For $T>T_\lambda$ the correlation length is ξ_+, given in Eq. (2.52), and for $T<T_\lambda$, the correlation length is ξ_T, Eq. (2.45b). The numerical value of A_∞ is discussed in Sec. III.

without the constraint. Since the computed spectra at T_c are non-Lorentzian one may define their characteristic frequencies in a number of different ways. The definition leading to (3.2), (3.3), (3.2a), and (3.3a) was in terms of the median frequency,[18] but one can also use the values $C_m(k,\omega=0)$ and $C_\psi(k,\omega=0)$.[9,10] We shall denote the corresponding ratios obtained using the latter definition by $R_m^{\rm crit}$ and $R_\psi^{\rm crit}$. The numerical values obtained for these are

$$R_m^{\rm crit}=0.31\,, \tag{3.2b}$$

$$R_\psi^{\rm crit}=0.31\,, \tag{3.3b}$$

with the constraint (2.22), and

$$R_m^{\rm crit}=0.42\,, \tag{3.2c}$$

$$R_\psi^{\rm crit}=0.27\,, \tag{3.3c}$$

without the constraint.

The parameter R_2 of II, which is the ratio of the half-width[11] of second sound at $k=\xi_T^{-1}$ to its frequency, is

$$R_2\equiv\frac{D_2\xi_T^{-1}}{2u_2}\approx R_\Gamma^\infty a_-^{1/2}(\bar\kappa\xi_T)^{-1/2}=0.09\,. \tag{3.4}$$

The above values of the amplitude ratios may be compared with the ϵ-expansion estimates obtained in I and II,

$$R_\lambda=(K_d/\epsilon)^{1/2}(1+0.6\epsilon)\approx 0.36\,, \tag{3.5}$$

$$R_{\psi}^{\rm crit}=(K_d/\epsilon)^{1/2}(1-0.3\epsilon)\approx 0.16\,, \tag{3.6}$$

$$R_{m}^{\rm crit}=(K_d/\epsilon)^{1/2}(1+1.4\epsilon)\approx 0.54\,, \tag{3.7}$$

$$R_2=(5)^{-1/2}(1+0.028\epsilon)(1/\xi_T\bar{\kappa})\approx 0.15\,. \tag{3.8}$$

In view of the erratic nature of the ϵ expansion, and of the variations introduced by the constraint (2.22), the order of magnitude agreement between (3.5)–(3.8) and the self-consistent values obtained in (3.1)–(3.4) must be considered satisfactory.

An alternative presentation of our results is in terms of the effective damping constant of second sound $D_2^{\rm eff}k^2$ for $T<T_c$, obtained from the full-width at half-maximum of the calculated peaks. In Fig. 3 we plot this width in units of Ω_∞ as a function of $k\xi_T$, up to the value $k\xi_T\approx 6$, beyond which the second-sound width is difficult to define. Similarly, for $T\approx T_c$ and $T>T_c$ we can obtain an effective thermal diffusivity $D_T^{\rm eff}$ from the half-width at half-maximum of the correlation function. This half-width is also plotted in Fig. 3 in units of Ω_∞, as a function of $k\xi_+$ above T_c, and for $10<k\xi_T<10^2$ below T_c. Of course these various parametrizations are only strictly valid in the limits $k\xi_T\ll 1$ or $k\xi_+\ll 1$, but they give a rough idea of the behavior for all $k\xi$. The second-sound frequency obtained from the Brillouin peak is also shown below T_c. A more complete representation of the data could be obtained by fitting the calculated correlation function to Eq. (2.25) at each value of $k\xi$ and plotting the functions $\bar{\lambda}(k,\xi)$, $\bar{\Gamma}(k,\xi)$, and $u_2(k,\xi)$ thus obtained.

B. Application to liquid helium

As explained in I, the variable m is the linear combination of entropy and mass density that enters second sound and thermal diffusion near T_c, and it is "orthogonal" to the pressure fluctuations which enter first sound. The function $C_m(k,\omega)$ is therefore proportional to the second-sound or thermal-diffusion contribution to the density correlation function $S(k,\omega)$.

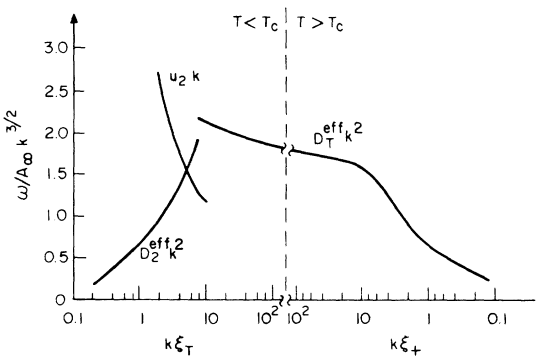

FIG. 3. Characteristic frequencies in the spectrum of $C_m(k,\omega)$, plotted as a function of $k\xi_T$ ($T<T_c$) and $k\xi_+$ ($T>T_c$). Below T_c the second-sound frequency u_2k and damping $D_2^{\rm eff}k^2$ (full-width at half-maximum) are shown. Near and above T_c the effective thermal-diffusion frequency $D_T^{\rm eff}k^2$ (half-width at half-maximum) is plotted.

In order to compare our calculation to experiment we must fix the nonuniversal frequency scale Ω_∞. As discussed in I, the principal difficulty one encounters in making such a determination is that the symmetric model we are using to describe helium can only be correct in an asymptotic limit where all transients have reached their critical value. A particularly slow transient is the specific heat $\chi_0=C_p$, which reaches a constant at T_c for $\alpha<0$, but is temperature dependent in the experimental range. Thus, strictly speaking, our calculations are only applicable for temperatures at which the measured values of $u_2\xi_T^{1/2}$ and $\lambda\xi_+^{-1/2}$ no longer vary. Since this range is never attained in practice, we must correct for the variation of the specific heat, at least approximately.

As was discussed earlier,[5,6,9] the most important effects of the slow transient may be taken into account at long wavelengths below T_λ by using the measured[22] second-sound velocity in Eq. (2.48), to define a temperature-dependent quantity

$$A_\infty(T)=R_\Gamma^\infty u_2(T)\xi_T^{1/2}\,. \tag{3.9}$$

Similarly, we can define a corresponding quantity above T_λ in terms of the measured[1] thermal conductivity and specific heat

$$A_\infty(T)=[\lambda(T)/C_p(T)]\xi_+^{-1/2}a_+^{-1/2}\,. \tag{3.10}$$

In order to generalize the above euqations to finite $k\xi$ we must be able to take into account the transients present at finite k and $T=T_\lambda$. To accomplish this we propose the following approximate scheme, which has the advantage that it is simple to carry out in practice. Near T_λ, the second-sound velocity may be written in the form [see Eq. (4.5) of I],

$$u_2(t)=u_2^0(t)(-t)^{\nu/2}\,, \tag{3.11}$$

where ν is the correlation exponent. In (3.11) we have used the slowly varying amplitude

$$u_2^0(t)=g_0/[\xi_T^0 C_p(t)]^{1/2}\,, \tag{3.12}$$

and the reduced temperature at the given pressure

$$t\equiv[T-T_\lambda(P)]/T_\lambda(P)\,. \tag{3.13}$$

The vertex g_0 is proportional to the entropy per particle $\sigma=S/R$ ($g_0=k_BT_\lambda\sigma/\hbar$), and $\xi_T=\xi_T^0(-t)^{-\nu}$ is obtained from the superfluid density by Eq. (4.4) of I (ξ_T was denoted κ_-^{-1} in I). Let us introduce a k-dependent effective temperature

$$t_-^*\equiv t[1+(k/\bar{\kappa})^2]^{3/4}=t[1+0.11(k\xi_T)^2]^{3/4}\,. \tag{3.14}$$

For $k\xi_T \ll 1$, t^* is proportional to $\xi_T^{-3/2}$, and for $k\xi_T \gg 1$, it goes as $k^{3/2}$. We define the effective second-sound velocity

$$u_2^*(k,t) \equiv u_2^0(t_-^*)(-t)^{\nu/2}, \tag{3.15}$$

by using t^* in place of t in (3.12b), and employ this in Eq. (3.9), so that we obtain an effective value of A_∞,

$$A_\infty(k,t) = R_\Gamma^\infty \xi_T^{1/2} u_2^*. \tag{3.16}$$

The use of this expression for the frequency scale $\Omega_\infty = A_\infty k^{3/2}$ below T_λ should yield a first approximation to the effects of the slow transients on the spectrum, for arbitrary values of $k\xi_T$.

Similarly, above T_λ, we may represent the measured thermal diffusivity as [see Eq. (4.21) of I],

$$D_T(t) = \lambda(t)/C_p(t) = R_\lambda g_0 [\xi_+^0/C_p(t)]^{1/2} t^{-\nu/2}, \tag{3.17}$$

and define

$$t_+^* \equiv t[1 + (k\xi_+)^2]^{3/4}, \tag{3.18}$$

and

$$D_T(t_+^*) = R_\lambda g_0 [\xi_+^0/C_p(t_+^*)]^{1/2} t^{-\nu/2}. \tag{3.19}$$

We then insert this expression into Eq. (3.10) and use

$$A_\infty(k,t) = D_T(t_+^*) \xi_+^{-1/2} a_+^{-1/2}, \tag{3.20}$$

in $\Omega_\infty = A_\infty k^{3/2}$ for finite k above T_λ.

The above scheme is of course only consistent to the extent that the R_λ extracted from experiment in (3.17) agrees with our value (3.1). More importantly, this scheme does not take into account various higher-order effects of the slow transients, which were discussed in Sec. IV B 3 of I. These lead, in particular, to a departure of the ratio $C_p(t)/C_p(-t)$ from its asymptotic value of unity, and to effects represented by the function $\varphi(\alpha_e)$ in Eq. (4.21) of I. We estimate these effects to introduce corrections of order 30%, which are within the accuracy of our calculations.

Let us note that the correlation function calculated in Fig. 2 is

$$\tilde{C}_m(k,z) \equiv \chi_0^{-1} C_m(k,\omega) \tag{3.21}$$

and is normalized by the condition

$$\int_0^\infty \tilde{C}_m(k,z)\, dz = \pi. \tag{3.22}$$

We thus obtain the physical correlation function $\chi_0^{-1} C_m(k,\omega)$, by changing the frequency scale from z to

$$\omega = z A_\infty k^{3/2}, \tag{3.23}$$

using Eqs. (3.16) and (3.20) for A_∞ at the appropriate values of k and T.

C. Comparison with experiment

The dimensionless ratios describing the hydrodynamic regime are R_λ and R_2, and these may be compared to macroscopic experiments. As mentioned earlier, the value $R_2 = 0.09$ given in (3.4) is roughly a factor[11] of 5 smaller than the experimental value $R_2^{\exp} = 0.5$, obtained from the second-sound damping.[2] The relevant ratio above T_λ is R_λ whose calculated value $R_\lambda \simeq 0.19$ is somewhat smaller than the experimental value[1] $R_\lambda^{\exp} \approx 0.3$ quoted in I. The discrepancy is in part due to the approximation (2.29) which replaces R_λ by the geometric mean of R_λ and R_Γ, and probably reduces R_λ, as is the case at T_λ [compare Eqs. (2.21) and (2.23)]. A similar effect would not seem to occur for R_2, since the damping of second sound arises from both $\bar{\Gamma}$ and $\bar{\lambda}$ below T_λ [see Eq. (2.28)], and the approximation (2.29) should not have as large an effect. Thus our calculations can be considered to agree with the long-wavelength experimental numbers above T_λ, but to disagree below T_λ. Similar results were found in the ϵ expansion.[9,10]

Turning to the light-scattering measurements,[3,4] we first obtain the frequency scale by noting that at $P = 23$ atm the second-sound velocity is given by[22]

$$u_2 = 1340(-t)^{1/3}[1 + 2.12(-t)^{1/6}] \text{ cm/sec}. \tag{3.24}$$

Although we have not analyzed (3.24) in terms of the measured C_p, we may use a procedure analogous to the one leading to (3.16) to find

$$\Omega_\infty = 7.1 \times 10^{-2}[1 + 2.12(-t_-^*)^{1/6}] k^{3/2} \text{ sec}^{-1}, \tag{3.25}$$

with k in cm^{-1}. This leads to the values

$$\Omega_\infty = 8.6 \times 10^6 \text{ sec}^{-1} \text{ for } T = T_\lambda,$$
$$k = 1.9 \times 10^5 \text{ cm}^{-1},$$

and

$$\Omega_\infty = 9.45 \times 10^6 \text{ sec}^{-1} \text{ for } T = T_\lambda - 1 \text{ mK},$$
$$k = 1.9 \times 10^5 \text{ cm}^{-1}.$$

From Fig. 3, we see that the normalized half-width at T_λ is 1.8, so the absolute value of the half-width in frequency units is

$$(2\pi)^{-1}\Omega_{1/2} = 2.5 \text{ MHz}, \quad k = 1.9 \times 10^5 \text{ cm}^{-1}, \tag{3.26}$$

which is larger than the value $(2\pi)^{-1} D_\kappa k^2 \approx 1.5$ MHz, reported by Vinen, *et al.*[4] (at $P = 20$ atm). Moreover, we expect (3.26) to be an underestimate, because of the constraint (2.23), and because the experiments must also include a background term. A preliminary comparison with data at T_λ by Tarvin *et al.*[7,23] for $k = 1.78 \times 10^5$ cm^{-1} and $P = 23$ atm, also leads to a similar discrepancy between experiment

and theory. Thus, although a more detailed comparison is advisable, it appears that our results disagree rather strongly with the finite-k measurements. In particular, we would have expected to see an increase in the thermal-diffusion width by at least a factor of 2, between $T = T_\lambda + 1$ mK and $T = T_\lambda + 0.05$ mK for wave vectors $k \approx 2 \times 10^5$ cm^{-1}, and no such variation has been found.[4,7,23] Similarly, we predict a marked temperature dependence in the second-sound width below T_λ at these wave vectors, which has also not been observed.[3,4,7]

We believe that these discrepancies, as well as the disagreement in the absolute value of R_2, represent deviations from the theory which are beyond the expected uncertainty of our calculations. We must therefore search for an explanation in terms of more fundamental corrections to the symmetric planar-spin model, than those already considered.

A correction which comes to mind is the presence of background terms, represented by λ_0 and Γ_0 in Eq. (3.20). These have to some extent been taken into account in determining the frequency scale (2.41), but their effect in Eq. (3.20) is clearly more complicated. In particular, such terms will yield corrections to the observed ratio R_2 which we have not taken into account. On the other hand, the background damping is still expected to scale as k^2 in going from the macroscopic measurements to the light scattering, as long as $k\xi_T < 1$. Such terms can therefore not fully explain the light-scattering data, although they might be important in quantitative comparison.

The enhanced damping of second sound at low frequencies suggests the presence of a slow relaxation process, which has not been taken into account. Such a process may in fact be significant in the asymmetric model (F) discussed in I, at finite temperatures below T_λ. In the asymmetric model, a second-sound wave couples linearly to the longitudinal fluctuations via the term $\gamma m |\psi|^2$ in F_0 [see Eqs. (2.16) and (3.9) of I], which is absent in the symmetric model. At low frequencies $\omega < u_2 \xi_T^{-1}$, and long wavelengths $k\xi_T < 1$, the longitudinal mode has a slow relaxation time, which might contribute significantly to the damping of second sound in this regime. For $\alpha < 0$, of course, the vertex γ has a vanishing fixed-point value, so this process may be neglected asymptotically close to T_λ. However, it represents an extremely slow transient, which decays as the effective exponent $\alpha_e(t)$ [see Sec. IV B 3 of I], and is not negligible in the experimental range. A crude estimate of the longitudinal relaxation rate τ_L^{-1} is obtained from the Ornstein-Zernike approximation (2.24), and yields

$$\tau_L^{-1} = \bar{\Gamma}\bar{\kappa}^2 \approx A_- \bar{\kappa}^{3/2}, \tag{3.27}$$

which is slower than the characteristic rate $u_2\bar{\kappa}$ entering in the intermediate propagators of the symmetric model, by a factor 3.6. Of course, the approximation (2.24) is highly unreliable at long wavelengths, since it is known[7] that the static susceptibility $\chi_L(k)$ diverges, and the longitudinal spectrum is certainly not Lorentzian. A more careful analysis of second-sound damping in model F, which takes these features into account, is therefore necessary in order to estimate the importance of the longitudinal relaxation.

Concerning the behavior at T_λ, the asymmetry corrections do not seem to be important, and we cannot account for the discrepancies. It is hoped that further experimental and theoretical work will clarify this issue.

ACKNOWLEDGMENTS

We wish to thank A. Kane for programming the numerical calculations, and A. Kornblit for help in the latter stages of the numerical work. We are indebted to G. Ahlers, T. Greytak, and J. Tarvin for discussions of the experimental situation.

---

*Supported in part by the NSF under Grant No. GH-34556.

[1]G. Ahlers, Phys. Rev. Lett. 21, 1159 (1968); in *Proceedings of the Twelfth International Conference on Low Temperature Physics*, edited by E. Kanda (Keigaku, Tokyo, 1971), p. 21.

[2]J. A. Tyson, Phys. Rev. Lett. 21, 1235 (1968).

[3]G. Winterling, F. S. Holmes, and T. J. Greytak, Phys. Rev. Lett. 30, 427 (1973); G. Winterling, J. Miller, and T. J. Greytak, Phys. Lett. A 48, 343 (1974).

[4]W. F. Vinen, C. J. Palin, J. M. Lumley, D. L. Hurd, and J. M. Vaughan, *Low Temperature Physics, LT-14*, edited by M. Krusius and M. Vuorio (North-Holland, Amsterdam, 1975), Vol. I, p. 191, and references therein.

[5]R. A. Ferrell, N. Menyhárd, H. Schmidt, F. Schwabl, and P. Szépfalusy, Phys. Rev. Lett. 18, 891 (1967); Ann. Phys. (N. Y.) 47, 565 (1968).

[6]B. I. Halperin and P. C. Hohenberg, Phys. Rev. 177, 952 (1969).

[7]T. Greytak, Bull. Am. Phys. Soc. 21, 424 (1976); and private communications.

[8]K. G. Wilson and J. Kogut, Phys. Rep. 12, 75 (1974).

[9]B. I. Halperin, P. C. Hohenberg, and E. D. Siggia, Phys. Rev. B 13, 1299 (1976), hereafter referred to as I.

[10]E. D. Siggia, Phys. Rev. B 13, 3218 (1976), hereafter referred to as II.

[11]Note that R_2, as defined in Eq. (7) of II is the ratio of the imaginary part of ω_2 to its real part. The imaginary

part of the frequency is the *half-width* of the line, or *one-half* the damping constant, so one should write $R_2 = D_2 \kappa_\perp^2 / 2u_2$, to conform to the usual convention for the definition of D_2. It is the R_2 defined in this way whose ϵ expansion is given in Eq. (7) of II. The experimental value quoted in II should be divided by 2, i.e., $R_2^{\text{expt}} \approx 0.5$.

[12]L. P. Kadanoff and J. Swift, Ann. Phys. (N. Y.) 50, 312 (1968).

[13]K. Kawasaki, Ann. Phys. (N. Y.) 61, 1 (1970).

[14]P. Résibois and M. DeLeener, Phys. Rev. 178, 806 (1969); D. A. Krueger and D. L. Huber, Phys. Lett. 33, 169 (1970).

[15]F. Wegner, Z. Phys. 218, 260 (1969).

[16]C. Joukoff, thesis (Université Libre de Bruxelles, 1974) (unpublished).

[17]P. C. Hohenberg, A. Aharony, B. I. Halperin, and E. D. Siggia, Phys. Rev. B 13, 2986 (1976).

[18]The "median" or "characteristic" frequency is defined in Eqs. (4.13)–(4.15) of Ref. 6.

[19]E. Brézin, D. J. Wallace, and K. G. Wilson, Phys. Rev. B 7, 232 (1973); E. Brézin and D. J. Wallace, *ibid.* 7, 1967 (1973); G. M. Avdeeva, Zh. Eksp. Teor. Fiz. 64, 741 (1973) [Sov. Phys.-JETP 37, 377 (1973)]; D. R. Nelson, Phys. Rev. B 13, 2222 (1976).

[20]G. G. Ihas and F. Pobell, Phys. Rev. A 9, 1278 (1974).

[21]R. Freedman and G. F. Mazenko, Phys. Rev. Lett. 33, 1575 (1975); and Phys. Rev. B 13, 4967 (1976).

[22]D. S. Greywall and G. Ahlers, Phys. Rev. A 7, 2145 (1973).

[23]J. Tarvin, F. Vidal, and T. J. Greytak, Bull. Am. Phys. Soc. 21, 354 (1976).